




Microplastic discharge from a wastewater treatment plant: long term monitoring to compare two analytical techniques, LDIR and optical microscopy while also assessing the removal efficiency of a bubble curtain

Patrick S. Bäuerlein ^{a,*}, Eelco N. Pieke ^b, Frank I. H. M. Oesterholt^a, Thomas ter Laak ^{a,c} and Stefan A. E. Kools ^a

^a KWR Water Research Institute, Nieuwegein, The Netherlands

^b Het Waterlaboratorium N.V., Haarlem, The Netherlands

^c Department of Freshwater and Marine Ecology (FAME), Institute for Biodiversity and Ecosystem Dynamics (IBED), University of Amsterdam (UvA), Science Park 904, Amsterdam, 1098XH, Netherlands

*Corresponding author. E-mail: patrick.bauerlein@kwrwater.nl

 PSB, 0000-0002-1110-5997; ENP, 0000-0001-8939-6264; TtL, 0000-0002-6182-6004; SAEK, 0000-0001-7257-0000

ABSTRACT

In this study we compare two parallel analytical methods while also testing a microplastics mitigation method. We assess the effectiveness of a bubble curtain to reduce microplastics in a wastewater treatment plant (WWTP)-effluent canal during the course of six months (>70 samples) using two analytical techniques: laser direct infrared (LDIR) and optical microscopy (OM) covering a size range of 0.02 to 5 mm. Comparison of the two analytical strategies shows similar trends, fluctuations, and correlating particle and fibre numbers. However, absolute values of particles differ, and the strategies provide different levels of information: LDIR is capable of identifying the plastic type as well as shape, while OM cannot determine the plastic type. Furthermore LDIR has a lower size limit (10–20 μm) than OM (50 μm). While information obtained by OM in general is far less detailed it is more affordable. This research also shows that the bubble curtain pilot does not have a measurable effect on the particle concentration. Possible effects of the curtain are hidden in the temporal variations. This research also reveals that individual samples show a large variation in particle numbers, illustrating that single measurements might give a poor representation of environmental particle number.

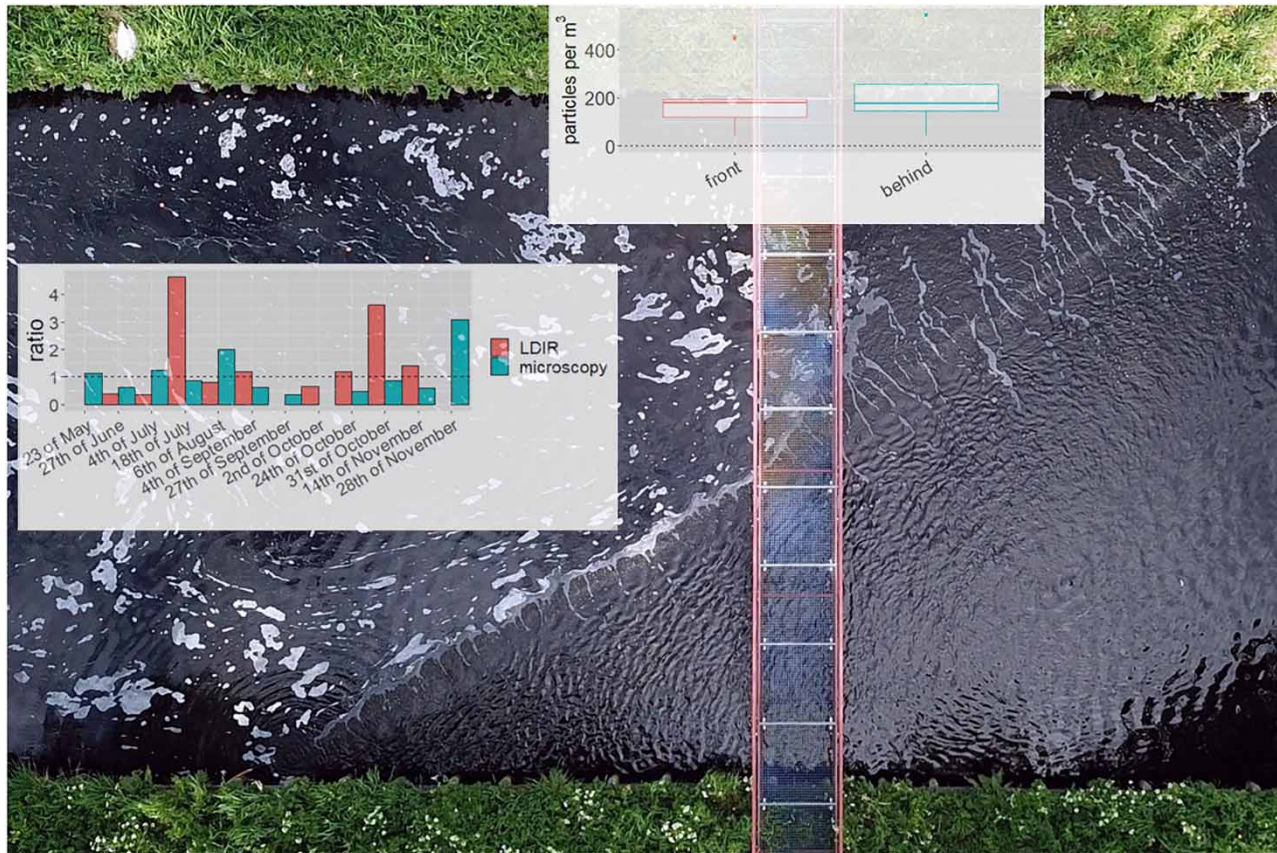
Key words: bubble curtain, LDIR, method development, microplastics, optical microscopy, sewage treatment plant

HIGHLIGHTS

- Effects of a bubble curtain on the microplastic concentration in the size range of 20 μm to 5 mm could not be detected.
- LDIR imaging and optical microscopy are complementary strategies for microplastic analysis.
- The sampling frequency and desired level of detail (e.g. type of polymer) determine the analysis method.
- Several measurements over time are necessary to get a clear picture of the microplastic concentration.

This is an Open Access article distributed under the terms of the Creative Commons Attribution Licence (CC BY-NC-ND 4.0), which permits copying and redistribution for non-commercial purposes with no derivatives, provided the original work is properly cited (<http://creativecommons.org/licenses/by-nc-nd/4.0/>).

GRAPHICAL ABSTRACT



INTRODUCTION

Plastics are only being produced on a larger scale since the 1950s. Yet, in 2018, the global production was 359 million tons of plastics annually, of which 62 million tons were produced in Europe alone (PlasticsEurope 2020). In environmental science the particle group of microplastics: plastic/polymer particles or fibres smaller than 5 mm but generally larger than $1 \mu\text{m}$ (Mintenig *et al.* 2018), are of special interest as an anthropogenic pollution of diverse matrices. Environmental microplastics are divided into two different major groups: primary and secondary microplastics. Primary plastics are produced as particles in the sub-millimetre size range (e.g. pellets) and may enter the environment via consumer products or losses during storage or transport. Secondary microplastics are the result of weathering and breakdown of all kinds of plastic products, including fibres from synthetic clothing, particles from tyre abrasion, weathering of plastic products, sports grounds and polymer paints (Woodall *et al.* 2014; Klein *et al.* 2018; Mintenig *et al.* 2018; Waldschläger *et al.* 2020).

From around 2014 onwards, research on microplastics was broadened to include freshwaters and terrestrial systems. These studies quickly showed how omnipresent microplastics are in a multitude of environmentally relevant matrices. By now, various studies have shown that plastics are detected in birds, fish, sediment, food, air and to some extent in (bottled) drinking water (Eriksen *et al.* 2014; Woodall *et al.* 2014; Dehaut *et al.* 2016; Rillig *et al.* 2017; Rodrigues *et al.* 2018; Brahney *et al.* 2021; Bäuerlein *et al.* 2022; Nizamali *et al.* 2023). There is also evidence that microplastics are vehicles for biofilm and can carry waterborne diseases (Mughini-Gras *et al.* 2021). Microplastics can also act as carriers of metals and chemicals (Carbery *et al.* 2018; Godoy *et al.* 2019).

One common source for microplastics in surface water is shown to be communal and industrial wastewater (Okoffo *et al.* 2019; Sun *et al.* 2019; Reddy & Nair 2022) from wastewater treatment plants (WWTPs). Although WWTPs do remove a large amount of plastic from the wastewater stream, especially larger particles, significant amounts can still be emitted from a WWTP and consequently end up in the environment (Iyare *et al.* 2020). Because WWTP-effluent is more effective at

capturing larger microplastics (>150 µm), the wastewater effluent likely contains an abundance of smaller particles which are considerably harder to analyse.

This study aims to elucidate the emissions of microplastics from one specific WWTP over a longer period of time. Additionally, we determine the efficiency of a bubble curtain as an additional post-treatment technique to retain microplastics. Bubble curtains may present themselves as a suitable option to remove microplastics as they are scalable, can treat large volumes of water, do not need chemicals and can be installed relatively easily (Ehrhorn 2017; TGBB 2021). These techniques could be employed as additional treatment step behind a conventional wastewater treatment plant without alteration of the treatment itself. Finally, this study compares the performance of optical microscopy with laser direct infrared (LDIR) spectroscopy, that employs a quantum cascade laser operating in the fingerprint region of the IR spectrum. While spectroscopic-based methods are able to give a comprehensive picture of microplastics, the costs may be prohibitive in large monitoring campaigns. Here, the objective is to show if a more cost-effective method such as microscopy is suitable for regular microplastic monitoring.

MATERIALS AND METHODS

Research location

We conducted this study at a municipal conventional WWTP Wervershoof, (Wervershoof, The Netherlands) containing a multiple-step treatment process: pre-sieving, aeration and sedimentation. The plant is operated by water board Hoogheemraadschap Hollands Noorderkwartier (HHNK). It has a capacity of 306.000 inhabitant equivalents and discharges on average 40 million litres a day. After sedimentation, treated effluent is discharged into an effluent canal that eventually runs off into Lake IJssel (IJsselmeer). The effluent canal is ca. 10 m wide and 1,500 m long. i. Lake IJssel has a Natura 2,000 status and serves as a drinking water source for the drinking water company (PWN) that supplies the province Noord Holland.

Installation and operation of the bubble curtain

The bubble curtain was installed in the effluent (outflow) canal of the WWTP, see Figure 1. The bubble curtain is created by pressurising air in a specifically designed tube made of perforated PVC, which is located on the bottom of the waterway. The bubble curtain creates an upwards thrust due to ascending air bubbles, which brings particulate matter and undissolved solids to the water surface. By placing it diagonally in the waterway, the bubble curtain uses the natural current to guide gathered matter to the catchment system at the riverside. In practice the system is fully functional when a catchment system is placed at the end of the bubble curtain to collect debris. However, a catchment system which catches plastics smaller than 1 mm has not been developed yet. Therefore, for this specific pilot research into microplastics, a catchment system was not installed. Plastic particles are intended to concentrate in front of the bubble curtain (Figure 1) in case the curtain works. Particle concentrations in front and behind the bubble will be compared. A significant higher concentration in front of the curtain is expected to prove that the curtain can be a viable abatement option for microplastics.

Sampling methods

Samples were taken at five locations on ten sampling dates (event) in the effluent canal between May and November 2019. Four locations are in proximity of the bubble curtain and named: 'upstream, front, behind, downstream'. Figure 1 shows

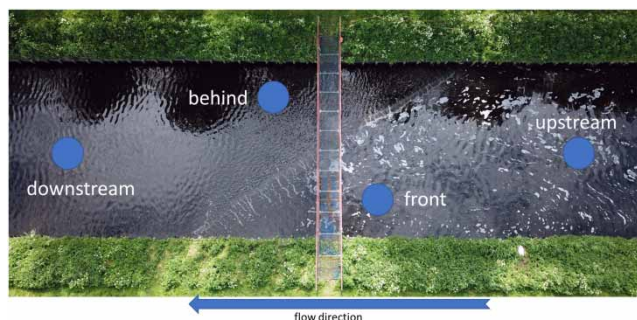


Figure 1 | Aerial picture of the working bubble barrier and the four sampling locations close to the barrier.

schematically four of these sampling points. The last sample point 'effluent' is located at the effluent discharge point of the WWTP and contains the direct effluent of the treatment plant. This sampling point is not shown in Figure 1. Location upstream was chosen to be 30 metres upstream from the bubble curtain and location downstream 30 metres downstream from the bubble curtain. The upstream point is approximately 100 metres from the discharge point. At these locations, no effects of turbulence from the bubble curtain or discharge were found and the stream was found to be in the baseline state. The 'front' point was selected based on pilot research by The Great Bubble Barrier (unpublished) showing the richest concentration of particles at this location (Figure 1). The 'behind' point was similarly selected indicating this point as the most lean concentration of particles under normal operating conditions.

At each sampling location two samples were taken per sampling event. One sample was processed for laser direct infrared (LDIR) analysis and one for microscopic analysis. However, as a maximum of eight samples could be logistically processed per sampling event, the number of available sample locations per sampling event was limited to four. Consequently, the location 'effluent' was sampled five times in the first phase of the research and was later replaced with sampling point 'downstream'.

Sampling depth was fixed at 15 cm below the water surface. To sample from the bridge above the bubble barrier a device was designed (Figure SI4 in Supplemental information) to ease the sampling and to ensure an equal sampling depth or both sampling devices. For the other two locations the sampling tube was fixated at the bank of the effluent canal.

The two methods, LDIR and microscopy, differ in the amount of water needed, sample treatment and data analysis. For both methods the individual steps are explained separately.

LDIR: 500 L of water was filtered through a cascade of two stainless-steel sieves (Gilson, USA) with mesh sizes of 500 μm and 100 μm followed by a 10 μm plankton net (Hydro-Bios, Germany) at the end. The 500 μm sieve was used to remove larger particles and to prevent clogging of the smaller sieves. Residue from the 500 μm -filter was not analysed. The other residues were later transferred into separate glass bottles using Milli-Q ultrapure water (Millipore Sigma, USA) and kept refrigerated at 4 °C until further sample pre-treatment.

Microscopy: 350 L to 600 L of water was filtered through a cascade of five stainless-steel sieves (Retsch, Germany) with mesh sizes of 50 μm , 125 μm , 250 μm , 1,000 μm , and 5,000 μm at a constant flux between 7–10 L/min for 1 hour. The smallest sieve (50 μm) was removed after 100 L (approximately 15 minutes) to prevent clogging. Sampling was stopped at the required volume or to prevent clogging of the 125 μm sieve. Exact volumes were recorded per sieve and used in subsequent concentration calculations. All sieves were sealed in aluminium foil and transported. Microplastics were recovered from the sieves into separate glass bottles using Milli-Q ultrapure water (Millipore Sigma, USA) and kept refrigerated at 4 °C until further sample pre-treatment.

Analytical methods: LDIR and microscopic method

The two methods applied in this research differ significantly in the identification and determination of size and shape of the plastic particles. (See Table 1). The microscopic method detects and characterises plastic particles visually. The LDIR with its quantum cascade laser detects and characterises particles based on their infrared light (IR) spectrum (Tian *et al.* 2022). The details of each method are given in this section.

Quality assurance

LDIR

Potentially contamination occurring during sample handling was minimised. All laboratory surfaces were cleaned with ethanol, equipment was rinsed and covered immediately with aluminium foil, and a cotton lab coat was worn at all times. Next to this, solutions of chemicals were filtered prior to use. Used materials were not made from plastic wherever possible (*e.g.*, a metal filter setup with a Teflon tube, the separation funnels made of glass). Negative controls were treated in parallel to each batch of actual samples to determine the degree of contamination. For the positive control a known number of plastic particles (green fluorescent PE, average diameter 100 μm) were added to a water sample. The percentage of particle number (PN) before and after work-up is the recovery rate. These control particles were counted visually under a microscope.

Microplastic measurements LDIR

Particle analyses were based on previously described methods (Mintenig *et al.* 2020; Mughini-Gras *et al.* 2021; Bäuerlein *et al.* 2022). Particle analysis focused on 10 μm and 100 μm residues of the sieves. The suspensions from these two fractions were

Table 1 | Details regarding the LDIR and microscopic methods

	LDIR method (KWR lab)	Microscopic method (HWL lab)
Sampling volume effluent	Approx. 500 L	Approx. 500 L
Sampling device filters	10, 100, 500 μm	50, 125, 250, 1,000, 5,000 μm
Size range covered	10–500 μm possible with the setup 20–500 μm measured and reported for the total PN number. Size fraction 10–20 μm was also measured for comparison reasons but not included in the total particle number count.	Larger than 50 μm
Size classification	Continuous: size is determined for each particle individually	Binned: particle is categorised based on the filter it was found on
Particle numbers	Determined in a subsample	Counted manually under a microscope
Particle colour	Cannot be determined	Determined visually
Particle shape	Determined based on physical parameters such as circularity, diameter etc.	Determined visually
Type of plastic	Determined by the software based on infrared spectra	Cannot be determined. Expert judgement used to assess if a particle is plastic or not

combined and filtrated over a 10 μm metal mesh. The filter was then transferred into a beaker with a 10% sodium dodecyl-sulfonate solution. After a day, the suspension was filtrated over a 10 μm metal mesh. The filter was then transferred into a beaker with 75 ml 12.5% potassium hydroxide solution and left standing for 5 days at 35 °C. Subsequently, the suspension was filtrated again through the same 10 μm metal filter. The residues were then transferred into a beaker with 50 ml 30% hydrogen peroxide solution and left standing for one day at 35 °C. The sample was filtrated again through the same metal filter, and the residues were transferred into a separation funnel using a 100 ml zinc chloride solution (1.6 g/cm³). The funnels were shaken and left standing to enable settling of denser materials. The settled material was discarded by continuously turning the valve of the funnel to prevent clogging, re-suspension and loss of plastics. About 10 mL of liquid was allowed to remain in the funnel. These 10 mL were filtrated again over a metal filter. Using 4 mL ethanol, the retained materials were removed from the filter and transferred into a glass vial. A vortex was created in this suspension to distribute the particles evenly. A subsample (2 × 50 μm) was taken and transferred on the microscope slide for analysis. From this subsample the actual particle number is extrapolated. The subsample is necessary as otherwise too many particles will be transferred onto the slide. The sample was analysed using an Agilent chemical imaging laser direct infrared (LDIR). Particles ranging from 20–500 μm were measured and quantified. If not stated otherwise particle numbers always mean particles in the size range from 20–500 μm per m³ sample. The smallest particles possible would be 3 μm , but as 10 μm was the smallest size-fraction collected, at no point particles smaller than 10 μm were scanned for. Four samples were analysed in parallel in combination with a negative control sample to detect (cross)-contamination during work-up and a sample spiked with a known amount of clearly visible fluorescent polyethylene microbeads (see quality control) to calculate the recovery rate. No negative control check was executed for the steps of sampling at the wastewater treatment plant in Wervershoof. After each set the whole equipment was cleaned using Milli-Q water and ethanol. The equipment was then covered with aluminium foil to prevent contamination from the air.

Microscopy

Clean-up of samples was kept as simple as possible as visual counting is not strongly influenced by background contamination. Each glass sample bottle containing different size fractions was concentrated separately by using a 30 μm stainless-steel mesh filter. The residue on the 30 μm mesh was back flushed with a minimal amount of prefiltered Milli-Q water into a separate glass beaker. Hence, for each sample, five beakers corresponding to five sieve fractions were prepared. To each sample 10 ml of 30% H₂O₂ was added and heated to 75 °C under constant stirring. Higher temperatures were chosen deliberately to reduce the amount of cellulose fibres (e.g. toilet paper) that may be mistakenly identified as microplastics. The solution was left to settle for at least 24 hours. After digestion, samples were again filtrated over 30 μm stainless-steel filters

and the residue was transferred using prefiltered Milli-Q water and separately vacuum filtered. The microplastics were transferred to a 0.45 µm bacterial cellulose nitrate (CN) filter on which subsequent analysis was performed (Sartorius Cellulose Nitrate filters, sterile, pore size 0.45 µm, green). Counting was performed on the CN-filters as these have a contrasting green background. For storage, the CN filters were kept wet and sealed from air under refrigerated conditions until analysis.

Analysis was performed with an Olympus stereomicroscope SZX10, magnification 6.3–63x, assisted by a light source (Photonische Optische Geräte, LED LichtquelleF3000). The CN filter was visually scanned for the presence of microplastics. If an uncertainty remained whether a particle was a plastic particle, metal tweezers were used to determine the fluidity and tension of the particle. Particles were classified as plastics if they were solid, not elastic, and able to resist tension force. Each confirmed microplastic particle was counted and categorised based on morphology; no size was recorded. At low numbers of microplastics, the entire filter was counted. If high levels of plastics were present, at least 10% of the filter was counted and the results extrapolated.

Data analysis

LDIR

Particle number: The particle number (PN) per sample is corrected for the number of particles in the negative control. These numbers are subtracted from the sample. Furthermore, the recovery rate from the positive control is applied to the particle number. E.g., a recovery rate of 90% means that the particle number of the sample is divided by 0.9.

Particle size/weight: Particle size was determined by the Agilent software based on the infrared image of the particle. The width and height of the particle were measured. The smallest dimension defines the category the particle belongs to. The third dimension was estimated based on a method used by Kooi *et al.* that enabled the calculation of a weight range from the volume of the particle (Kooi & Koelmans 2019; Sun *et al.* 2019). The lower limit of the plastic mass and the upper limit of plastic mass of all measurements were taken and used for the calculation of the minimum and maximum daily discharge of the WWTP. Because of the large variance between the lowest and the highest possible mass, an average using all the samples was calculated.

Chemical characterisation: The particles were identified by the Agilent software (Clarity).

Particle shape and colour determination: Particle colour cannot be determined by this method. The particle shape of the identified particles was determined using the Random Forest Model package (Breiman and Cutler's Random Forests for Classification and Regression – Version 4.6-14) in R (Breiman *et al.* 2020). The particles were split into six categories (sphere, particle, rod, fibre, fibre/cluster and artefact). Example pictures of each class can be found here (Table SI2 in the supplemental information). About 500 different particles were categorised and this data set was used to identify the shapes of the other particles. Variables defining the category of particles were diameter, aspect ratio, area, perimeter, eccentricity, circularity, solidity and the maximum IR adsorption.

Statistical analysis: Column statistics were performed using GraphPad Prism 5.01. ANOVA (analysis of variation), Shapiro–Wilk test and t-test were performed in R (v. 1.2.1335) from stats package 3.6.1. For *p*-values a threshold of 0.05 was used.

MICROSCOPY

Size classification: Particles were assigned a size fraction based on the filter on which they were found. The sieve on which the particle was found defines the size category. Particle size was not measured for each particle individually. E.g., a particle found on a 50 µm sieve, will be binned as a particle of 50–125 µm in size, regardless of its actual size. This approach was chosen as measuring the size of each particle individually would have been too time-consuming.

Particle number: The amount of microplastics per sieve size was counted. The CN-filter is divided into 144 units in a grid. Depending on the number of microplastics on the filter, it was partially counted (at least 15 units) or completely counted. If the collection filter was counted completely, the total amount of plastics was used as-is. If the collection filter was partially counted, results were extrapolated to account for the entire collection. To express it as volume-based unit, the total amount of plastics was corrected for the sampling volume.

Particle colour and shape: Microplastics were binned based on morphological qualities (colour, shape, and size). Each individual microplastic particle was assigned a shape category and colour category. The following shape categories were defined: sphere, rod, miscellaneous and fibre. The following colour categories were defined: white, grey-white, black, blue, green, yellow, red, and miscellaneous.

Dataset: Due to the binning methods applied for size, shape, and colour, each analysis resulted in a combination of 55 parameters consisting of bins size, shape, and colour combinations. The total number of parameters is smaller than possible combinations, as not all combinations are compatible or found (e.g., red rods). Per parameter the total number of microplastics corresponding to that classification was reported. The data was visualised using 2D and 3D plots.

Weather conditions and water flow rate from the WWTP

The weather conditions for each of the sampling dates were retrieved from the KNMI (The Royal Dutch Metrological Institute, Table SI1 in Supplemental Information). The closest measuring station is in Berkhout, about 14 km southwest of WWTP Wervershoof. In addition, a weather station was mounted on top of the bubble curtain generator. The flow in the WWTP was monitored (Figure SI1 in Supplemental Information). Selected sampling dates had variable weather conditions. For analysis, dates with sewer overflow were excluded as this would not reflect emissions under standard operating conditions. Such a date was November 28th. The rain resulted in a severe overflow. Results were excluded from analysis but were used to (qualitatively) evaluate the impact of sewer overflow on emissions. The data from this day were not included when calculating averages. The change of speed and direction of the wind may also have an impact on particle numbers at the sampling locations as water can be pushed back or the water can be churned up. However, as there is no clear pattern in the weather data, the possible impact of the wind was acknowledged but not substantiated.

Chemicals

LDIR: The following chemicals were purchased: Sodium dodecylsulfonate from Merck (Darmstadt, Germany), KOH from Merck (Darmstadt, Germany), H₂O₂ (30%) from Boom, ZnCl₂ from Boom (Meppel, The Netherlands), Ethanol from Boom (Meppel, The Netherlands), fluorescent green polyethylene microspheres from Cospheric (Santa Barbara, USA), Milli-Q water with >18 MΩ from Veolia (The Netherlands). All liquids used, including the cleaning liquids, were filtered prior to usage over 5 μm sieves and stored in closed bottles. These liquids were exclusively used for microplastic research. All equipment was at all times covered when not used to prevent air contamination, except when the samples were taken on location.

Microscopy: The following chemicals were purchased: stabilised hydrogen peroxide (Merck, 30%). Demineralised water was produced in-house. Liquid chemicals were filtered over 30 μm mesh filters before usage.

RESULTS AND DISCUSSION

Outflow of WWTP

As a first step the direct effluent was analysed for the presence of microplastics. In order to be able to assess the removal efficacy of the bubble curtain, a particle count of >1,000 per m³ is desired. The outflow of the WWTP Wervershoof from the effluent discharge point and from the beginning (sample point upstream) of the canal (Figure 1) were analysed to see if plastic particles were present. The average outflow was observed to be between ca. 4,000 (>50 μm) and 48,000 particles per m³ (>20 μm) (Figure 2), depending on the analysis method and selected size range in the effluent and canal. The presence of plastic particles at these levels justified to install the bubble curtain as a means to remove plastic particles from the canal.

Effectiveness of the bubble curtain

To test the efficacy of the bubble curtain, samples were taken at two positions (front and behind) close to the curtain (Figure 2).

To test whether the bubble curtain successfully retains microplastic particles, two hypotheses were formulated:

1. The ratio of particle numbers between the front and the back of the bubble curtain should be significantly greater than one if more particles accumulate in front of the curtain/barrier.
2. Larger particles are more easily trapped in front of the bubble curtain than smaller particles.

To test the first hypothesis, the ratios of the particle numbers between the two sampling points were calculated for each individual day. If the barrier retains particles of all sizes equally, the ratio should be larger than one because particles will accumulate in front of the curtain. The ratios and box plots for the microscopy and LDIR data are shown in Figure 3. A one-way t-test showed that the ratio on average is not significantly larger than 1 (*p*-value = 0.14 (LDIR) and 0.38 (microscopy)). Our observation is that the overall particle number at different sampling points is not affected measurably

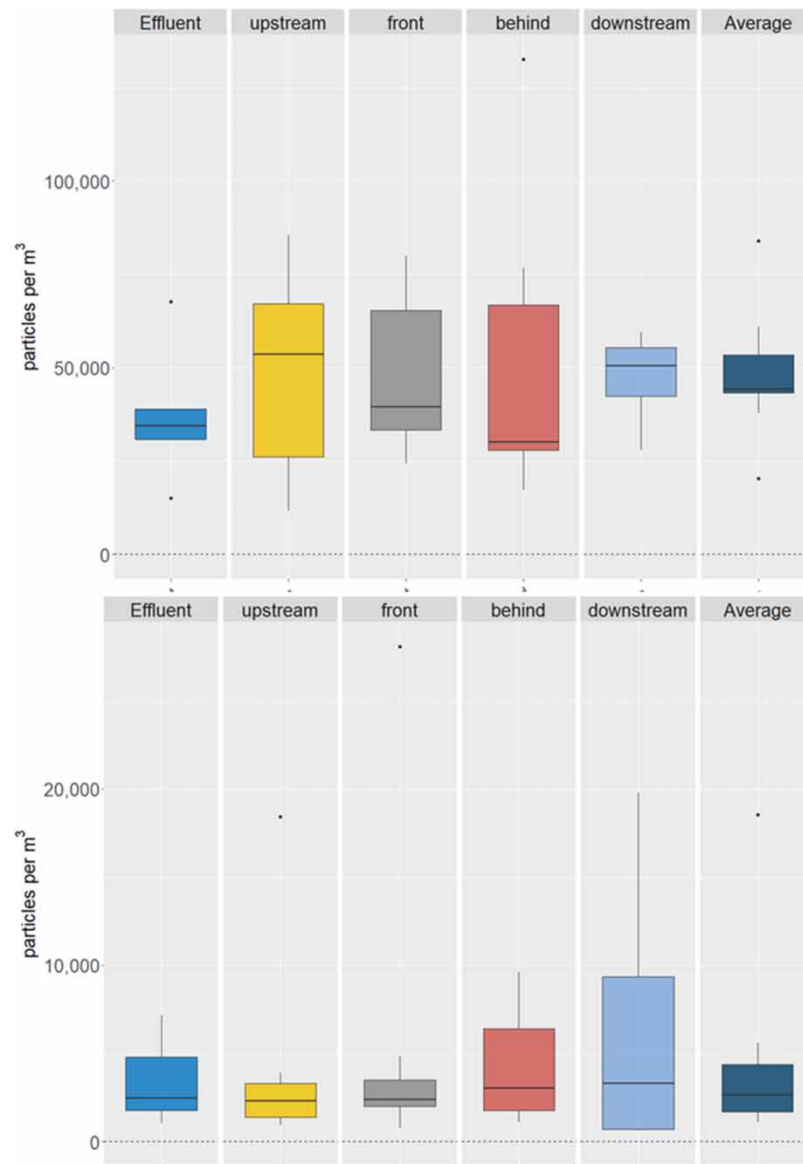


Figure 2 | From top to bottom. Average particle concentration measured with the LDIR, Average particle concentrations measured using microscopy.

by the curtain. This still leaves the possibility that certain size fractions or particle types are affected by the barrier despite the fact that the total numbers do not show a significant difference.

To evaluate the size distributions at the different sampling locations and the potential effect of the bubble curtain on the size of the microplastics, the size distributions were evaluated on both sides of the bubble curtain locations and compared (Figure SI6 and SI7 both in the Supplemental information). This was done by using linear regression on the log-log transformed data (size vs relative abundance). A significant change in the slope would indicate that the size distribution did change. Slopes of the two sampling points were calculated and compared. Comparison of the same-day slopes of front and behind shows that there is no significant difference between the size distributions (Table SI3 and SI4 both in the Supplemental information). The pooled slopes for the two sampling points also support this as there is no significant difference between before and after the barrier (LDIR: -2.04 ± 0.31 (front) and -1.67 ± 0.25 (behind), microscopy: -0.61 ± 0.27 (front) and 0.64 ± 0.19 (behind)).

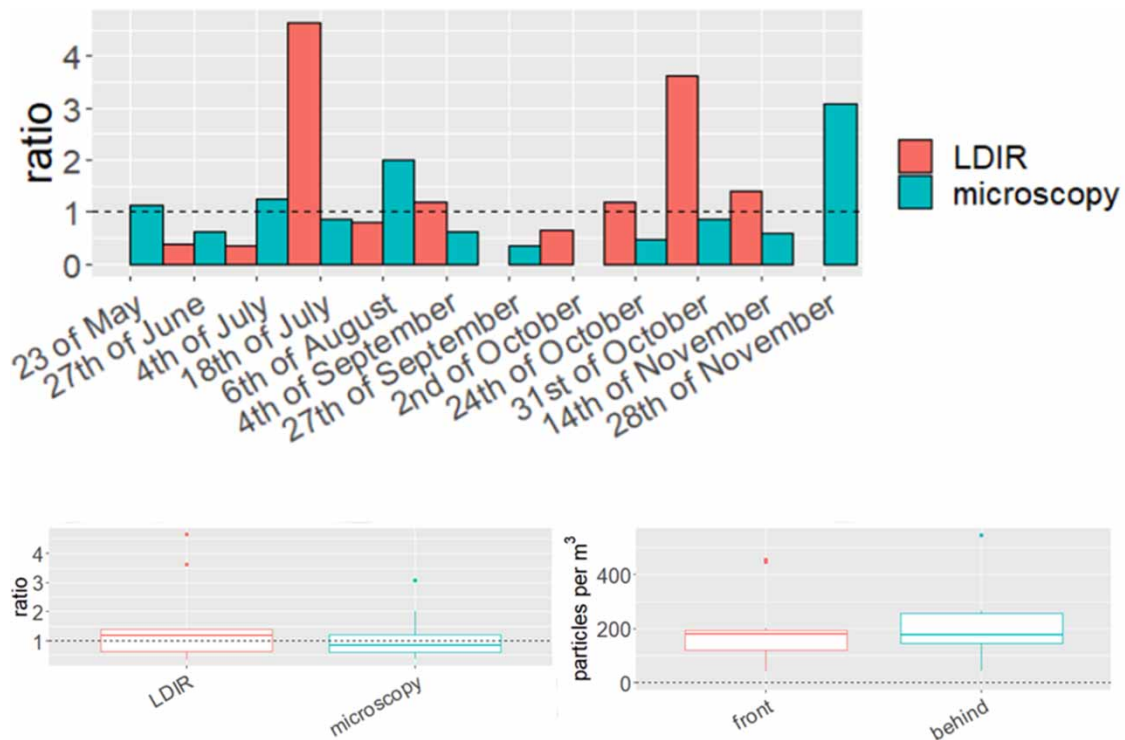


Figure 3 | Ratios of all particles between the locations, front and behind for the LDIR and microscopy data and the particle concentration for particles (top and bottom left). Particle number (1,000–5,000 μm) front and behind the curtain measured with the microscopic method (bottom right).

As the smaller particles are more numerous these will weigh heavy on the slope of the fitted trend line and therefore minor changes in larger particle numbers might go undetected. Therefore, particle numbers of the larger particles ($>1,000 \mu\text{m}$) were looked at more closely. Earlier research with the bubble barrier showed that it can effectively remove larger floating micro-particles ($>1 \text{ mm}$) from streaming water (Ehrhorn 2017; TGBB 2021). However, Figure 3 (bottom right) shows that there is no significant difference between the particle concentration in front of the barrier and behind for the size fraction 1,000 to 5,000 μm in this study.

This means that based on these data, there is neither an effect on the removal of plastic particles over the whole tested size range, nor an effect for specific size classes.

There are a number of reasons that may explain why the effectiveness of the bubble curtain could not be measured. Firstly, it is possible that too few particles in the size range of $>1 \text{ mm}$ were available to recognise a measurable difference by the bubble curtain. Secondly, another explanation could be that the bubble curtain cannot remove particles and fibres smaller than 1 mm at 15 cm depth, instead working only for buoyant larger plastic fragments at surface level. In earlier experiments several buoyant objects (e.g. buoyant bottles and polystyrene foam, but also foils in suspension bags, cups and polystyrene foam) and particles between 1 and 5 mm were successfully removed (up to 98%) using a bubble curtain (unpublished data).

Finally, external effects such as current, wind direction, convection, or the flow of the water in the effluent canal may have nullified any impact of the bubble curtain. Testing the bubble curtain under more controlled conditions in a laboratory setting could help to answer whether a bubble curtain is effective for microplastics under controlled conditions.

Plastic release from the WWTP (all sampling points)

As the bubble curtain had no measurable effect on the plastic concentration in the canal, all sampling points have been pooled to get a better picture of the total plastic particle number and types of plastic in the effluent and canal.

We noted that total particle numbers vary between sampling points and days. Our results show that the WWTP releases a consistent number of particles per day (Figure 2, Figure 5, and Figure SI8 in the Supplemental information). These numbers can differ significantly between sampling points and days. The larger variation in day-to-day (Figure 6) data underlines the

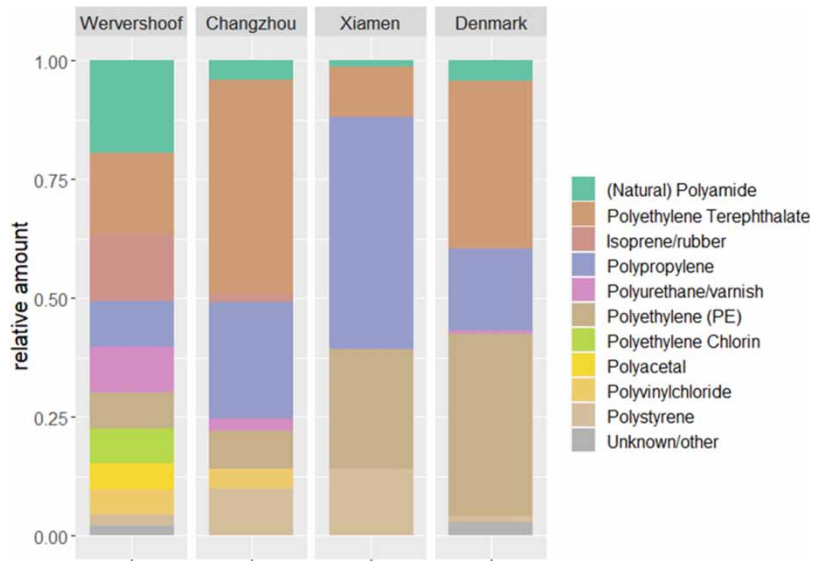


Figure 4 | Relative abundance of the 10 most abundant plastics in WWTP Wervershoof compared to three WWTPs (Simon *et al.* 2018; Long *et al.* 2019; Xu *et al.* 2019).

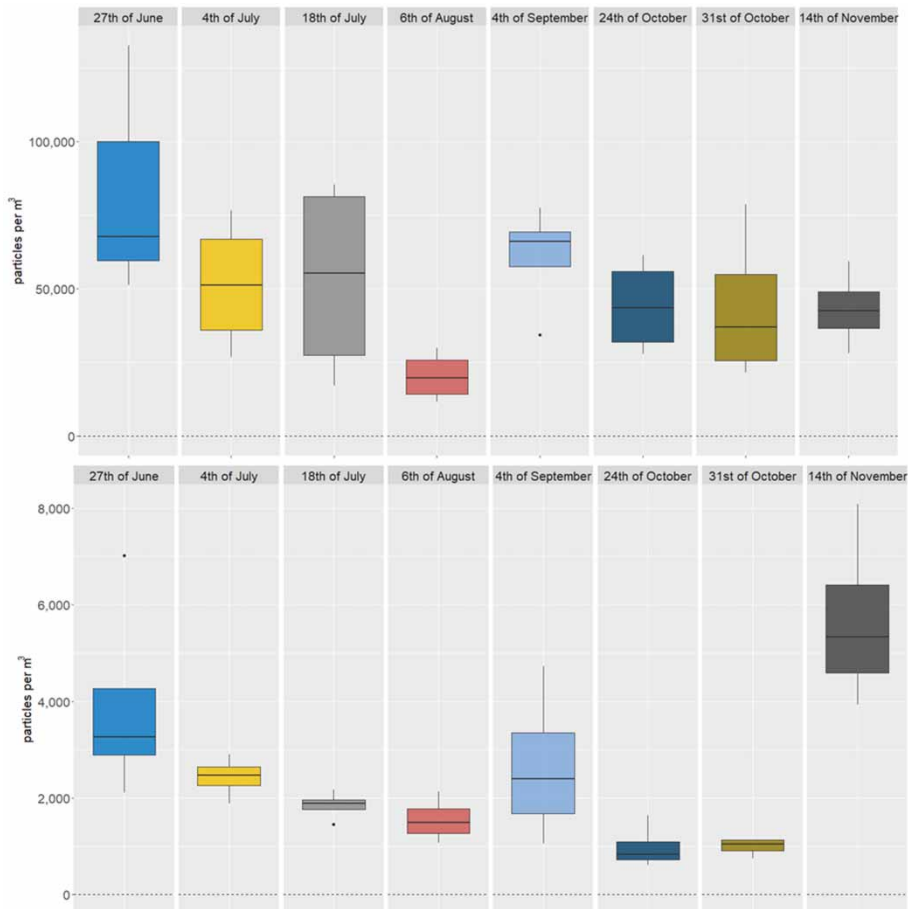


Figure 5 | LDIR (top) and microscopic method (bottom) averages per day.

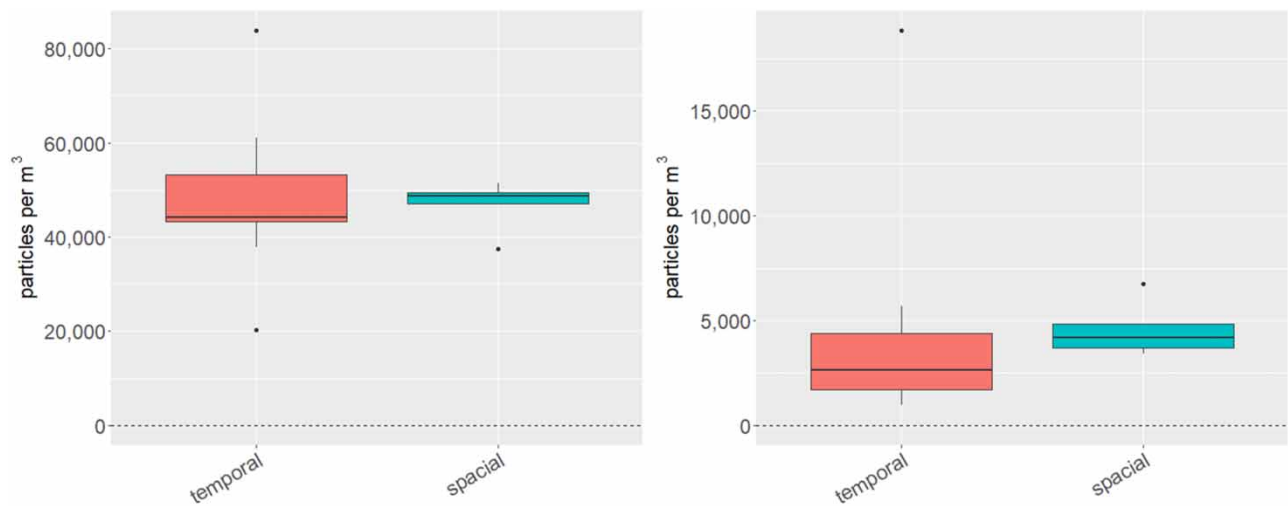


Figure 6 | Variance of particle numbers for LDIR (left) and the microscopy method (right). Temporal: Average of each day's average. Spatial: Average of each locations average.

Table 2 | Calculated discharge from WWTP Wervershoof

	LDIR method	Microscopy method
Average PN/m ³	~48,000	~4,000
Average PN/year	7*10 ¹¹	5*10 ¹⁰
Maximum mass discharge kg/year	~19	n.d.
Average plastic fibres/m ³	1,000–2,000	1,000–2,000

necessity that a sufficient number of samples needs to be taken to get a meaningful particle number on average for a certain location.

The total discharge of microplastics into the environment can be estimated using all data collected from this WWTP. Based on LDIR data, on average about 48,000 particles are in one cubic metre of effluent water (Table 2). This is in accordance with findings from Simon *et al.* (2018), who reported 19,000 to 477,000 p/m³ from particles from 10 µm upwards. The 48,000 p/m³ corresponds to about 700 billion particles per year being discharged into the environment from this particular WWTP (40 million L of water per day). With the microscopy method about 4,000 particles per cubic metre are found which means an outflow of about 58 billion particles per year. The data from the microscopy can be compared to a few studies and shows that particle numbers are comparable taking into account that size brackets are not exactly the same. A WWTP in Glasgow (UK) released about 250 MP per m³ (>65 µm) (Murphy *et al.* 2016) and one WWTP in the East Midlands (UK) released about 1,500 MP per m³ (>54 µm). These calculations do not take into account that an overflow can occur that can change the numbers significantly.

Overall, studies show that particle numbers fluctuate by several orders of magnitude in various WWTPs around the world (Iyare *et al.* 2020; Schmidt *et al.* 2020). Particle numbers as low as 0.7 p/m³ (USA) and as high as 54,000 p/m³ (Denmark) can be found, so finding large variations between experimental results at different WWTP sites is not uncommon. The numbers are impacted by a large number of factors including the size range that is being investigated, the analytical method and the type of WWTP. Hence, due to the lack of standardised methods it is difficult to compare results between studies. This problem has been recognised before (Schmidt *et al.* 2020; Kirstein *et al.* 2021).

Applying the discharge from Wervershoof to the 0.5–11.9 mg/m³ from Simon *et al.* would result in an emission of 7 to 173 kg microplastics per year. This means, under the assumption that the daily discharge is the same, the amount of microplastic discharged on a yearly basis is comparable (Table 2). Given that WWTPs relatively efficiently remove microplastics from the effluent (99%) (Sun *et al.* 2019; Xu *et al.* 2019; Iyare *et al.* 2020), this means that ca. 1,900 kg of microplastics at

WWTP Wervershoof is removed annually. This estimation is based on the microplastics found in the size range 20–500 µm, however, as larger particles that are likely to arrive at the WWTP and contain relatively more mass, the actual mass of removed plastics is likely much higher. Large plastic fragments are e.g. already removed by the sieves on intake and other plastic particles may be retained in the WWTP processes.

For the specific fibre discharge, both methods detected levels between 1,000 and 2,000 fibres/m³ effluent. This is much lower than recently reported fibre numbers in WWTP effluents (22,000 ± 18,000 p/m³) (Athey *et al.* 2020). Nevertheless, our data suggest that on a daily basis, about 80 million fibres are released (Michielssen *et al.* 2016). This number is in range of reported fibre numbers in literature (21,000 to 153.4 billion); however, the range of reported values is sizeable. The lowest fibre discharge is reported from a WWTP in Sweden, the highest from a WWTP in Russia. For larger size fractions > 50 µm studied by microscopy in this report, the majority of particles are fibres. This is also in accordance with the literature which shows that between 60 and 90% of all the particles found in effluent are fibres (Iyare *et al.* 2020).

The fraction of polymers identified in the investigated WWTP, as shown in Figure 4, is compared with recent studies that investigated similar samples. In the WWTP Wervershoof the most abundant polymer found was polyamide (PA, 18%). The other polymers that were found predominantly were PET, Isoprene, PU/varnish, PP, and PE-Cl, PE. These polymers are commonly found in effluents or surface waters (Mintenig *et al.* 2020). In total 27 different types of polymers were found. Two percent of the particles found in the samples could not be attributed to any polymer type.

The variation between relative particle number distributions in the table can be explained by the fact that different WWTPs received different influent depending on the plastic usage in their vicinity. The presence of PA is especially notable, as this is more than expected from the literature, which estimates 1–3%. One possible explanation could be that there is still organic material in the sample that did not break down completely during the chemical digestion. As a result, these particles were counted as microplastics composed of natural PA.

METHOD COMPARISON

Current progress in microplastic analysis shows that comparability between methods is often poor, as minor changes in methodology can greatly influence results. This can be seen e.g. when comparing data from various WWTPs (Iyare *et al.* 2020) or in drinking water research (Kirstein *et al.* 2021). The amount and type of microplastics found depend greatly on both the sampling process (e.g., lower size, sample pre-treatment) as well as the analytical process (e.g., counting, identification). In this study, two different methods were used to maximise the span and scope of the particles. In this section, the methods are compared in more detail.

Total particle number

Particle numbers (PN) found with the LDIR method are significantly higher in all samples than the particle numbers from the optical microscope method. This was expected as the LDIR method can detect particles down to 20 µm whereas the microscopic method is limited to 50 µm particles. It is well known that smaller particles are more abundant (Kooi & Koelmans 2019). In addition, the microscopic method used a rigorous clean-up at elevated temperatures to minimise the presence of cellulose fibres and to ensure mostly microplastics are counted, which comes at the cost to likely decrease the total number of microplastics in analysis. For the LDIR method on average between 25,000–60,000 particles per m³ were found for the various locations and with the microscope between 1,000–6,000 particles per m³ were found (Figure 2).

Despite the differences in methods, a similar trend between sample events is found by both methods (Figure 5). Figure 6 also shows that scattering of the data is larger between different dates than it is between the different locations. This is true for both methods.

Particle numbers per size fraction

As shown, particle numbers of the two detection methods cannot be compared directly due to the different size limitations. Therefore the particle counts (all measurements) from the two methods were categorised to match the size categories of the optical microscope method (Figure 7). The total particle count of the 50–125 size range is a factor 10 higher for the LDIR method. This difference can be explained by the fact that a 50 µm sieve was the lower limit during sampling for microscopy, whereas for the LDIR method 10 µm was the lower limit. It is known that particles with an elongated shape can pass through sieves if the orientation permits, e.g., a long 1,000 µm particle may be able to pass through a 200 µm sieve if the width of the particle is smaller than 200 µm (Lehtiniemi *et al.* 2018). Therefore, because a 50 µm sieve does not exactly cut off at 50 µm

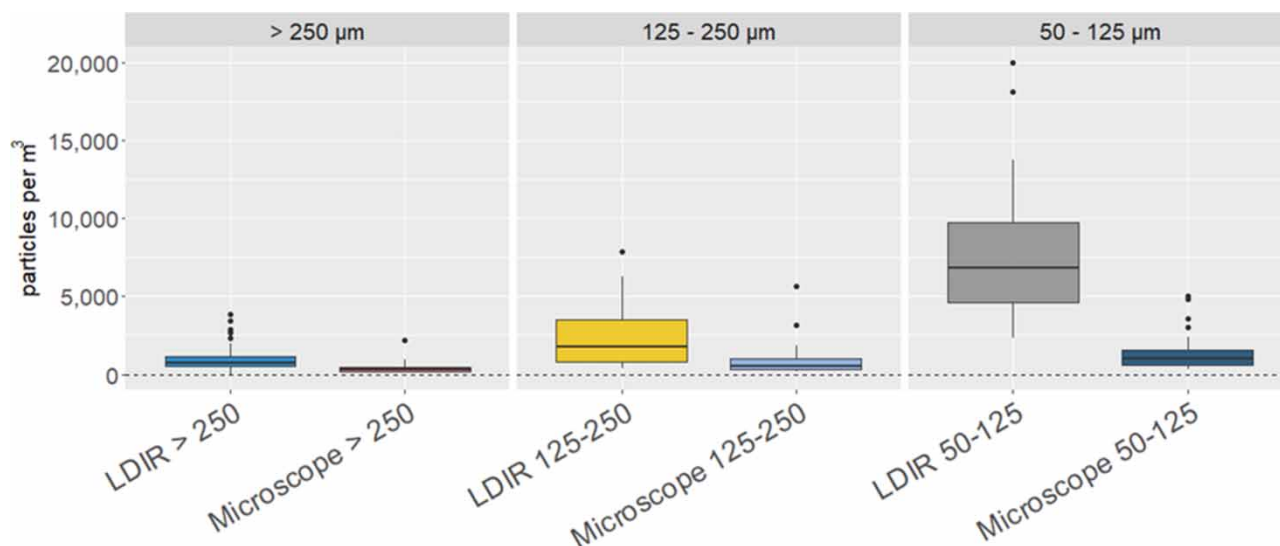


Figure 7 | Comparison of the average particle number from all dates and locations for the different size classes measured with the two different methods. Sizes are in micrometres.

there is a realistic probability that particles of 50 µm may pass through that sieve, causing an underestimation. For the LDIR method the lower sieve size is smaller (10 µm), so 50 µm particles are likely to be retained. A lower bound underestimation can also be observed for LDIR when comparing 10 to 20 µm particles. In five cases the PN for 20 µm particles was larger and in the other cases the numbers were almost equal or slightly more for 10 µm particles. Hence, it appears that the closer a particle size is to the smallest filter mesh used, the higher the chance that PNs get underestimated. This means that it is crucial that not only the measured particle sizes are mentioned but also the smallest mesh size used for sampling as well as work-up.

In addition, particles can be missed during visual counting, which will likely lead to bias towards large particles and fibres or rod-shaped particles that might be easier recognised as plastics (Kooi & Koelmans 2019). For example, a plastic particle that visually appears as a sand particle will be excluded in the visual microscopic method but included in the LDIR spectroscopic method. Additionally, the differences in categorisation of particles with the two methods can also explain the difference. In the LDIR method the smallest dimension defines the size class of the particle, whereas in the optical microscope method the sieve on which the particle was found determines the size class. Hence, especially for fibre-like particles the classification between the two methods differs greatly.

Looking at the other size classes the difference between the two methods is less pronounced. The particle numbers in the size range of 125–250 µm are slightly higher for the LDIR method, but the difference is not as profound as for the 50–125 µm size range ($p = 0.05$). The slightly higher counts of particles might be explained by the different definition of size of the two methods (see materials and methods). For the larger size range (>250 µm) no significant difference was observed ($p = 0.23$) and relative differences became smaller. The LDIR size fraction contains slightly more particles on average although the upper limit is 500 µm, whereas the upper limit for the microscopy method is 5,000 µm.

All samples from LDIR and microscopy show that with increasing particle size, the particle number decreases. This is in accordance with earlier findings (Kooi & Koelmans 2019). To assess the correctness of this correlation, log-log plots for all LDIR and microscopy measurements were made and the quality of the linear regression was evaluated (Table 3 and Figure SI3 in Supplemental information).

LDIR: With LDIR, performance characteristics improve when the upper size range is reduced as relatively few larger particles are found. Detection of larger particles is, due to their smaller number, much more affected by chance, so removing these from the regression reduces the variation. Choosing a smaller overall size distribution for the linear regression also inevitably comes along with a bias for the smaller particles. However, as 95% of all the particles in this dataset are between 20–200 µm, fitting between 20 and 200 µm using 10 µm steps while ignoring larger particles is optimal. The value of the slope in this regression is -2.14 ± 0.41 , which coincides with a reported average value of -1.6 ± 0.5 (Kooi & Koelmans 2019). Particle numbers sized 200 µm and larger can be calculated based on extrapolating using the formula from the linear regression.

Table 3 | Calculated slopes and quality parameters for the linear regression of the log-log plots

Size range	Pooled slope	Pooled R ²	Pooled Sy.x
LDIR	Steps of 10		
20–490	-1.66 ± 0.31	0.84	0.24
20–200	-2.14 ± 0.41	0.90	0.20
20–100	-2.28 ± 0.43	0.92	0.15
LDIR	20–50 then steps of 50		
20–490	-2.13 ± 0.41	0.95	0.18
MICROSCOPY			
50–5,000	-0.66 ± 0.23	0.84	0.25
50–1,000	-0.91 ± 0.34	0.96	0.13

These results are decent, as shown when applying this method for data from the 4th of July upstream sample point. With the LDIR method actual PN larger than 200 μm is 1,392 particles while calculation yields a PN between 2,404 and 3,180.

MICROSCOPY: Regression of these data cannot be based on particle size, because only binned data are collected per size fraction as recording particle size per particle is too inaccurate and time-consuming. The linear regression reveals that microscopy also has an underestimation of the larger particles. This can be seen once particles larger than 5,000 μm are also included: the R² value drops from 0.96 to 0.84 and the Sy.x rises from 0.13 to 0.25. It should be noted that the generally high R² value (0.96) for microscopy is based on a linear regression with only four size categories. The calculated slope for regression based on microscopy data is smaller than the average reported in the literature (-1.6 ± 0.5).

In both data sets there appears to be a negative bias on the lowest size fraction. As explained, the closer a particle size is to the smallest filter mesh used, the higher the chance that PNs pass through the filter and are underestimated in counting. Furthermore, smaller particles are more prone to biofouling and hetero-aggregation which will result in deposition in the environment (Kooi *et al.* 2016, 2017). Should these small particles have been in the effluent, this could explain their absence in the sampling device.

Particle shape and fibre numbers

Particle shape was determined differently for the two methods. With the microscopy method particles are detected and characterised visually and with the LDIR method a particle is labelled based on physical parameters (see materials and methods). For both methods the relative amount of particle shape differed (Figure 8). With microscopy the dominant microplastic species are identified as fibres in 75% of the cases. For LDIR the relative abundance of fibres lies between 2–4% and mainly particles, spheres, and rods are found. This difference is supported by a recent study on a sewage treatment plant (WWTP) in Changzhou (Xu *et al.* 2019), where fibres are dominant in sizes $>100 \mu\text{m}$ and fragments or rods are dominant in sizes $<100 \mu\text{m}$. As fibres are usually larger particles, with the exception of fibre/clusters (Figure SI5 in the Supplemental information), they are expected to be less abundant in the smaller size fraction. Smaller particles are less prone to be fibres as the maximum possible ratio between thickness and length is limited for small particles.

Total fibre numbers determined by the two methods were compared (Figure 9 and Figure SI2 in the Supplemental information). Both LDIR and microscopy find similar quantities of fibres in the samples. On average approximately between 1,000 and 2,500 fibres per m^3 were found for all locations. The ratio of the two methods (t-test) per location shows that only for the effluent the diversion from 1 is significant ($p = 0.09$).

The overall comparison between the applied methods (microscopy and LDIR) indicates that the methods show similar trends and comparable results. However, there are obviously significant differences. The LDIR method finds more particles on average. Trends with regard to WWTP- and bubble curtain hypotheses are similar and give the same results. Day-to-day variation between methods was similar. In addition, PN in comparable size classes are similar with similar trends, and the number of fibres detected is proportional. Excess particles were detected by both methods for dates with heavy rainfall and sewer overflow. The most obvious difference between the methods is found when size distributions are compared. Comparison of the slopes shows that the microscopy method underestimates the smaller size fraction, whereas the LDIR method

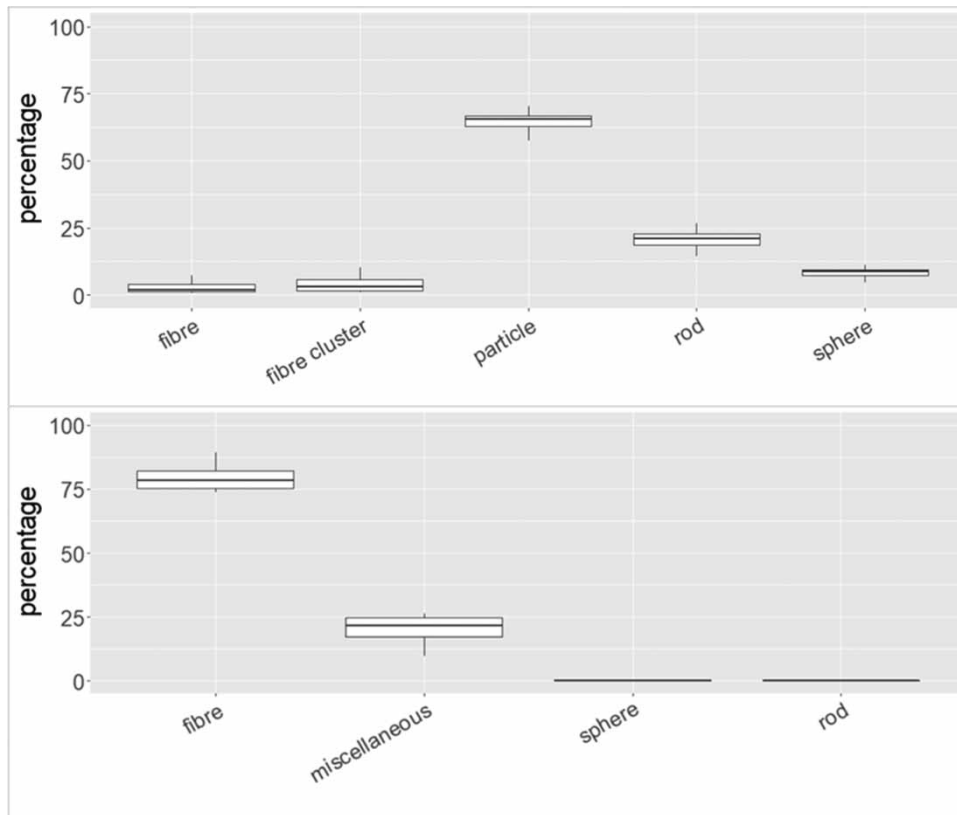


Figure 8 | Relative abundance of different particle shapes (Top: LDIR – size range 20–500 μm), Bottom: microscopy – size range (50–5,000 μm).

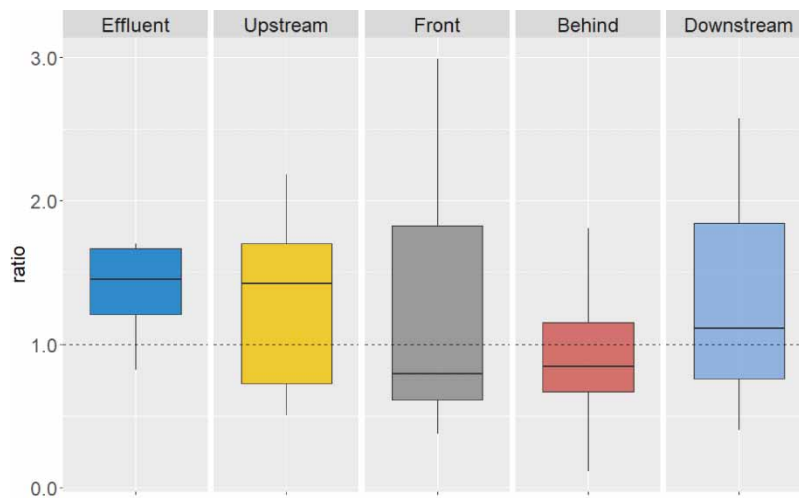


Figure 9 | Fibre concentration per location and date and the ratio LDIR/microscopy for the different locations.

is prone to underestimation of the larger size fractions. The latter can also be a consequence of the size definition and/or of the fact that few large particles are found and hence extrapolation can bias the results. Consequently, size regression slopes of these two methods are significantly different.

It must be noted that comparing results from literature sources with results from this study or with other literature results is not a straightforward comparison. As mentioned, selected sample strategies, applied sampling devices, the measuring technique and types of plastics that can be detected have a significant impact on the measured particle number or their size classification. These differences can readily reach one order of magnitude. Hence, relating values from one study to another study is precarious and, so far, has not been demonstrated to be successful. The medley of sampling and analytical methods that comes along with wildly distributed particle numbers is well documented (Sun *et al.* 2019).

Expressing the discharge of microplastics in mass units is especially prone to error: not only will the different methods influence this number but also the way how the mass was calculated or estimated. For example, to calculate the mass the density and the volume of the particles must be determined which includes assumptions that will inevitably be different between various studies and algorithms.

Despite the difficulty comparing literature results, the method performance in this study is on par with that in literature results, fortifying these findings. In conclusion, the presented methods appear to be sufficiently comparable. This means the much cheaper microscopic method can be a viable alternative for the more expensive, however, also considerably more sophisticated LDIR methods, if larger microplastics (>50 µm) need to be monitored on a frequent basis. In general it can be said that the sample amount and size range should determine the method. This opinion coincides with an earlier expressed opinion by Song *et al.* (2015).

CONCLUSIONS

This study focuses on the potential removal of microplastics and the analysis of microplastics between 20 and 5,000 µm in a wastewater effluent stream. Here, we show that a bubble curtain is not able to demonstrably remove microplastic particles. The data of the bubble curtain setup show that changes in concentration between upstream and downstream of the curtain are indistinguishable from temporal variations at all sampling points. These temporal variations also demonstrate that a single sample is not adequate and that sampling over longer periods of time is necessary to get a good picture of the actual particle emissions, especially considering that extreme weather events strongly influence the measurements. Heavy rainfall and sewer overflow cause an excess of particles detected by both methods LDIR and optical microscopy.

This study shows LDIR and optical microscopy are complementary techniques for determination of microplastics and show similar trends with regard to particle concentration. Comparison of the two methods also demonstrates that the LDIR method is suitable when detailed information is needed, e.g., for smaller particles and for each individual particle (exact size, type polymer). The microscopic method can also be a viable method to reduce the costs of the analysis if the focus is mainly on larger particles and no detailed information on the nature of the particles is needed. However, the microscopic method is not suitable for smaller particles (<50 µm) and suffers from particle concentration underestimation in the lower size regions.

It also must also be noted that comparing results from the literature with results from this study is not a straightforward comparison. Selected sample strategies, applied sampling devices, the measuring technique and types of plastics that can be detected have a significant impact on the measured particle number and/or their size classification. These differences can easily reach one order of magnitude or more. Hence, relating values from one study to another study is precarious and, so far, has not been demonstrated to be successful. The authors suggest having a table accompanying each study with the most important information such as filter size, size measured, sample volume.

ACKNOWLEDGEMENT

The authors want to thank The Great Bubble Barrier (TGBB), Hoogheemraadschap Hollands Noorderkwartier (HHNK), PWN and PWN Technologies (PWNT) for their help in this project. We also want to thank the Topconsortia for Knowledge & Innovation (TKI) of the Ministry of Economic Affairs and Climate for funding this research.

FUNDING

This activity is co-financed with TKI funding from the Top consortia for Knowledge & Innovation (TKIs) of the Dutch Ministry of Economic Affairs. Others members of the consortium are: PWN, PWNT, HHNK and TGBB.

DATA AVAILABILITY STATEMENT

All relevant data are included in the paper or its Supplemental Information.

CONFLICT OF INTEREST

The authors declare there is no conflict.

REFERENCES

- Athey, S. N., Adams, J. K., Erdle, L. M., Jantunen, L. M., Helm, P. A., Finkelstein, S. A. & Diamond, M. L. 2020 The widespread environmental footprint of indigo denim microfibers from Blue Jeans. *Environmental Science & Technology Letters* **7** (11), 840–847.
- Bäuerlein, P. S., Hofman-Caris, R., Pieke, E. N. & ter Laak, T. 2022 Fate of microplastics in the drinking water production. *Water Research* **221**, 118790.
- Brahney, J., Mahowald, N., Prank, M., Cornwell, G., Klimont, Z., Matsui, H. & Prather, K. A. 2021 Constraining the atmospheric limb of the plastic cycle. *Proceedings of the National Academy of Sciences* **118** (16), e2020719118.
- Breiman, L., Cutler, A., Liaw, A. & Wiener, M. 2020 randomForest: Breiman and Cutler's Random Forests for Classification and Regression.
- Carbery, M., O'Connor, W. & Palanisami, T. 2018 Trophic transfer of microplastics and mixed contaminants in the marine food web and implications for human health. *Environment International* **115**, 400–409.
- Dehaut, A., Cassone, A.-L., Frère, L., Hermabessiere, L., Himber, C., Rinnert, E., Rivière, G., Lambert, C., Soudant, P., Huvet, A., Duflos, G. & Paul-Pont, I. 2016 Microplastics in seafood: benchmark protocol for their extraction and characterization. *Environmental Pollution* **215**, 223–233.
- Ehrhorn, P. 2017 *Anpassung Einer Druckluftsperr zur Reduzierung von Mikro- und Makroplastik aus Fließgewässern*. Technische Universität Berlin Berlin.
- Eriksen, M., Lebreton, L. C. M., Carson, H. S., Thiel, M., Moore, C. J., Borerro, J. C., Galgani, F., Ryan, P. G. & Reisser, J. 2014 Plastic pollution in the world's oceans: more than 5 trillion plastic pieces weighing over 250,000 tons afloat at sea. *PLOS ONE* **9** (12), e111913.
- Godoy, V., Blázquez, G., Calero, M., Quesada, L. & Martín-Lara, M. A. 2019 The potential of microplastics as carriers of metals. *Environmental Pollution* **255**, 113363.
- Iyare, P. U., Ouki, S. K. & Bond, T. 2020 Microplastics removal in wastewater treatment plants: a critical review. *Environmental Science: Water Research & Technology* **6** (10), 2664–2675.
- Kirstein, I. V., Gomiero, A. & Vollertsen, J. 2021 Microplastic pollution in drinking water. *Current Opinion in Toxicology* **28**, 70–75.
- Klein, S., Dimzon, I. K., Eubeler, J., Knepper, T. P., 2018 In: *Freshwater Microplastics: Emerging Environmental Contaminants?* (Wagner, M. & Lambert, S. eds.). Springer International Publishing, Cham, pp. 51–67.
- Kooi, M. & Koelmans, A. A. 2019 Simplifying microplastic via continuous probability distributions for Size, Shape, and Density. *Environmental Science & Technology Letters* **6** (9), 551–557.
- Kooi, M., Reisser, J., Slat, B., Ferrari, F. F., Schmid, M. S., Cunsolo, S., Brambini, R., Noble, K., Sirks, L. A., Linders, T. E. W., Schoeneich-Argent, R. I. & Koelmans, A. A. 2016 The effect of particle properties on the depth profile of buoyant plastics in the ocean. *Scientific Reports* **6**, 33882.
- Kooi, M., Van Nes, E. H., Scheffer, M. & Koelmans, A. A. 2017 Ups and downs in the ocean: effects of biofouling on vertical transport of microplastics. *Environmental Science and Technology* **51** (14), 7963–7971.
- Lehtiniemi, M., Hartikainen, S., Nääki, P., Engström-Öst, J., Koistinen, A. & Setälä, O. 2018 Size matters more than shape: ingestion of primary and secondary microplastics by small predators. *Food Webs* **17**, e00097.
- Long, Z., Pan, Z., Wang, W., Ren, J., Yu, X., Lin, L., Lin, H., Chen, H. & Jin, X. 2019 Microplastic abundance, characteristics, and removal in wastewater treatment plants in a coastal city of China. *Water Research* **155**, 255–265.
- Michielssen, M. R., Michielssen, E. R., Ni, J. & Duhaime, M. B. 2016 Fate of microplastics and other small anthropogenic litter (SAL) in wastewater treatment plants depends on unit processes employed. *Environmental Science: Water Research & Technology* **2** (6), 1064–1073.
- Mintenig, S. M., Bäuerlein, P. S., Koelmans, A. A., Dekker, S. C. & Van Wezel, A. P. 2018 Closing the gap between small and smaller: towards a framework to analyse nano- and microplastics in aqueous environmental samples. *Environmental Science: Nano* **5** (7), 1640–1649.
- Mintenig, S. M., Kooi, M., Erich, M. W., Primpke, S., Redondo- Hasselerharm, P. E., Dekker, S. C., Koelmans, A. A. & van Wezel, A. P. 2020 A systems approach to understand microplastic occurrence and variability in Dutch riverine surface waters. *Water Research* **176**, 115723.
- Mughini-Gras, L., van der Plaats, R. Q. J., van der Wielen, P. W. J. J., Bauerlein, P. S. & de Roda Husman, A. M. 2021 Riverine microplastic and microbial community compositions: a field study in The Netherlands. *Water Research* **192**, 116852.
- Murphy, F., Ewins, C., Carbonnier, F. & Quinn, B. 2016 Wastewater treatment works (WwTW) as a source of microplastics in the aquatic environment. *Environmental Science & Technology* **50** (11), 5800–5808.
- Nizamali, J., Mintenig, S. M. & Koelmans, A. A. 2023 Assessing microplastic characteristics in bottled drinking water and air deposition samples using laser direct infrared imaging. *Journal of Hazardous Materials* **441**, 129942.

- Okoffo, E. D., O'Brien, S., O'Brien, J. W., Tscharke, B. J. & Thomas, K. V. 2019 Wastewater treatment plants as a source of plastics in the environment: a review of occurrence, methods for identification, quantification and fate. *Environmental Science: Water Research & Technology* **5** (11), 1908–1931.
- PlasticsEurope. 2020 Available from https://www.plasticseurope.org/application/files/6315/4510/9658/Plastics_the_facts_2018_AF_web.pdf.
- Reddy, A. S. & Nair, A. T. 2022 The fate of microplastics in wastewater treatment plants: an overview of source and remediation technologies. *Environmental Technology & Innovation* **28**, 102815.
- Rillig, M. C., Ziersch, L. & Hempel, S. 2017 Microplastic transport in soil by earthworms. *Scientific Reports* **7** (1), 1362.
- Rodrigues, M. O., Abrantes, N., Gonçalves, F. J. M., Nogueira, H., Marques, J. C. & Gonçalves, A. M. M. 2018 Spatial and temporal distribution of microplastics in water and sediments of a freshwater system (Antuã River, Portugal). *Science of the Total Environment* **633**, 1549–1559.
- Schmidt, C., Kumar, R., Yang, S. & Büttner, O. 2020 Microplastic particle emission from wastewater treatment plant effluents into river networks in Germany: loads, spatial patterns of concentrations and potential toxicity. *Science of the Total Environment* **737**, 139544.
- Simon, M., van Alst, N. & Vollertsen, J. 2018 Quantification of microplastic mass and removal rates at wastewater treatment plants applying focal plane array (FPA)-based Fourier transform infrared (FT-IR) imaging. *Water Research* **142**, 1–9.
- Song, Y. K., Hong, S. H., Jang, M., Han, G. M., Rani, M., Lee, J. & Shim, W. J. 2015 A comparison of microscopic and spectroscopic identification methods for analysis of microplastics in environmental samples. *Marine Pollution Bulletin* **93** (1), 202–209.
- Sun, J., Dai, X., Wang, Q., van Loosdrecht, M. C. M. & Ni, B.-J. 2019 Microplastics in wastewater treatment plants: detection, occurrence and removal. *Water Research* **152**, 21–37.
- TGBB. 2021 Available from <https://thegreatbubblebarrier.com/>.
- Tian, X., Beén, F. & Bäuerlein, P. S. 2022 Quantum cascade laser imaging (LDIR) and machine learning for the identification of environmentally exposed microplastics and polymers. *Environmental Research* **212**, 113569.
- Waldschläger, K., Lechthaler, S., Stauch, G. & Schüttrumpf, H. 2020 The way of microplastic through the environment – application of the source-pathway-receptor model (review). *Science of the Total Environment* **713**, 136584.
- Woodall, L. C., Sanchez-Vidal, A., Canals, M., Paterson, G. L. J., Coppock, R., Sleight, V., Calafat, A., Rogers, A. D., Narayanaswamy, B. E. & Thompson, R. C. 2014 The deep sea is a major sink for microplastic debris. *Royal Society Open Science* **1** (4), 140317.
- Xu, X., Jian, Y., Xue, Y., Hou, Q. & Wang, L. 2019 Microplastics in the wastewater treatment plants (WWTPs): occurrence and removal. *Chemosphere* **235**, 1089–1096.

First received 15 June 2022; accepted in revised form 13 December 2022. Available online 20 December 2022